Electronic Supplementary Material (ESI) for Inorganic Chemistry Frontiers.

Electronic Supplementary Information

α-$LiMB_9O_{15}$ (M = Sr, Pb): Flexible [B_3O_7] Units Leading to the Low Temperatures Phase of β-$LiMB_9O_{15}$ (M = Sr, Pb)

Kaitong Liu,[a, b] Jian Han,*[, a, b] Fuming Li,[a, b] Shujuan Han,[a, b] Zhihua Yang,[a, b] Xuping Wang,*[, a] and Shilie Pan*[, a , b]

[a] CAS Key Laboratory of Functional Materials and Devices for Special Environments, Xinjiang Technical Institute of Physics & Chemistry, CAS; Xinjiang Key Laboratory of Electronic Information Materials and Devices, 40-1 South Beijing Road, Urumqi 830011, China.

[b] Center of Materials Science and Optoelectronics Engineering, University of Chinese Academy of Sciences, Beijing 100049, China

* Corresponding authors: hanjian@ms.xjb.ac.cn, wangxp@sdas.org, slpan@ms.xjb.ac.cn.

2. Experimental Section

2.1 Synthesis.

α-$LiSrB_9O_{15}$ polycrystalline powders were prepared by solid-state reaction. The stoichiometric ratio of Li_2CO_3, $SrCO_3$, and H_3BO_3 were weighed and ground evenly. The evenly ground mixture was slowly heated from room temperature to 450 °C and held for 10 hours, then slowly heated to 770 °C and held at this temperature for 7 days. During the holding period, the mixture was ground several times. The purity of the polycrystalline powders was determined by powder XRD tests. Millimeter-sized single crystal of α-$LiMB_9O_{15}$ (M=Sr, Pb) was obtained by the high-temperature melt method. For α-$LiSrB_9O_{15}$, it is obtained under a closed system. The reagents of LiF, SrF_2, and B_2O_3 were weighed with a molar ratio of 4:2:7. These raw materials were mixed thoroughly and loaded into the quartz tube. The tube was sealed at the vacuum degree of 10^{-3} Pa and then placed in the Muffle furnace. It was slowly heated to 600 °C and held for 10 hours, and cooled to 500 °C at the rate of 1 °C/h. Then it was decreased to 400 °C at 2 °C/h and finally cooled rapidly to 30 °C. Finally, small transparent grains were obtained. For α-$LiPbB_9O_{15}$, the molar ratio of LiF, PbF_2, and B_2O_3 is 3:1:15. The platinum crucible was placed in a temperature-controlled single crystal furnace and heated to 630 °C at a rate of 100 °C /h. At this time, all the solid reactants were melted. After holding 10 h at this temperature, the temperature was cooled to 530 °C at a rate of 2 °C /h. It was then lowered to room temperature at a rate of 10 °C/h, and the colorless crystals were obtained. Unfortunately, the polycrystalline of α-$LiPbB_9O_{15}$ can not be obtained by changing experimental strategies.

2.2 Structural Characterization.

The resulting millimeter-sized single crystals were used for data collection, single-crystal diffraction data of α-$LiMB_9O_{15}$ (M=Sr, Pb) were collected on a Bruker D8 Venture diffractometer using monochromatic Mo *K*α radiation at room temperature. The initial crystal structures were solved by the direct method and then refined with anisotropic displacement parameters for all atoms using the SHELXTL program package.[1] The structures were verified by PLATON and no higher symmetry elements were found.[2] Crystal data and structure refinement information are given in **Table 1**. The final refined atomic positions, isotropic thermal parameters, and bond valence sum (BVS) calculations of the atoms are summarized in **Tables S1**, **S2**. Selected bond distances (Å) and angles (deg) are listed in **Tables S3**, **S4**.

2.3 Powder X-ray Diffraction.

Powder XRD patterns were used to test the purity of the polycrystalline. An automated Bruker D2 Phaser X-ray diffractometer equipped with a diffracted beam monochromator set for Cu *K*α radiation (λ = 1.5418 Å) was used at room temperature in the angular range of 2θ = 10-70 º with a scan step width of 0.02 º and a fixed counting time of 1 s/step.

2.4 Infrared Spectroscopy.

Infrared spectroscopy was carried out on a Shimadzu IR Affinity-1 Fourier transform infrared spectrometer with a resolution of 2 cm^{-1} in the 400-4000 cm^{-1} range at room temperature. KBr was used as the reference pellet and the samples were

mixed thoroughly with it.

2.5 UV−Vis−NIR Diffuse Reflectance Spectroscopy.

UV–vis–NIR diffuse-reflectance spectroscopy data in the wavelength range of 180–1600 nm was recorded at room temperature using a powder sample on a Shimadzu SolidSpec-3700 DUV spectrophotometer.

2.6 Thermal Analyses.

Thermal gravimetric analysis (TGA) and differential scanning calorimetry (DSC) were carried out on a simultaneous NETZSCH STA 449 F3 thermal analyzer instrument in a flowing N_2 atmosphere.

2.7 Computational Methods.

The first-principles calculations were performed by the plane-wave pseudopotential method implemented in the CASTEP software package.[3] The exchange-correlation potential was calculated using Perdew-Burke-Ernzerhof (PBE) functional within the generalized gradient approximation (GGA).[4] To achieve energy convergence, the kinetic energy cutoff of 820 and 940 eV for α-$LiMB_9O_{15}$ (M=Sr, Pb) within normal-conserving pseudopotential (NCP) was adopted, respectively.[5-6] The Monkhorst–Pack *k*-point meshes in the Brillouin zone were set as 3 × 3 × 4 and 4 × 4 × 4 for α-$LiMB_9O_{15}$ (M=Sr, Pb), respectively. Based on the band structure, the linear optical refractive indices and birefringence can be obtained by the real part of the dielectric function.

Table S1. Atomic coordinates ($\times 10^4$), equivalent isotropic displacement parameters ($Å^2 \times 10^3$), and BVS of each atom for α-$LiSrB_9O_{15}$. U(eq) is defined as one-third of the trace of the orthogonalized U_{ij} tensor.

Atoms	x	y	z	U(eq)	BVS
Li(1)	4921(11)	2410(20)	4997(7)	20(2)	1.16
Sr(1)	7402(1)	7482(1)	6582(1)	15(1)	2.10
B(1)	2443(8)	4746(6)	5331(4)	13(1)	3.05
B(2)	546(8)	6799(8)	5250(4)	14(1)	3.03
B(3)	72(7)	9645(8)	5288(5)	13(1)	3.12
B(4)	2361(8)	10862(7)	6038(4)	14(1)	3.01
B(5)	234(8)	9991(8)	6969(5)	15(1)	3.03
B(6)	-74(7)	9518(8)	8701(4)	14(1)	3.08
B(7)	2703(8)	8264(7)	8668(4)	14(1)	2.98
B(8)	4844(7)	6395(7)	8367(5)	13(1)	3.13
B(9)	4776(7)	9005(7)	7656(4)	10(1)	2.99
O(1)	3956(4)	4377(4)	5217(3)	12(1)	2.12
O(2)	1457(4)	3884(4)	5849(3)	11(1)	1.97
O(3)	1880(5)	6083(5)	4928(3)	18(1)	2.20
O(4)	240(5)	8156(5)	4848(3)	17(1)	2.02
O(5)	-297(5)	6104(5)	5931(3)	17(1)	2.03
O(6)	1534(5)	10501(5)	5287(3)	15(1)	1.95
O(7)	3906(4)	11154(5)	5949(3)	15(1)	2.03
O(8)	1632(5)	10808(5)	6883(3)	17(1)	2.01
O(9)	-486(5)	9415(5)	6215(3)	16(1)	2.10
O(10)	-438(5)	9632(5)	7756(3)	19(1)	1.98
O(11)	1191(4)	8429(5)	8894(3)	14(1)	2.08
O(12)	3480(5)	9443(5)	8178(3)	17(1)	1.98
O(13)	3489(5)	6934(4)	8870(2)	12(1)	1.96
O(14)	5312(4)	7508(6)	7698(2)	18(1)	2.25
O(15)	5527(5)	9915(5)	7063(3)	17(1)	2.04

Table S2. Atomic coordinates ($\times 10^4$), equivalent isotropic displacement parameters ($Å^2 \times 10^3$), and BVS of each atom for α-$LiPbB_9O_{15}$. U(eq) is defined as one-third of the trace of the orthogonalized U_{ij} tensor.

Atoms	x	y	z	U(eq)	BVS
Li(1)	10000	10000	9160(30)	11(3)	1.23
Pb(1)	6667	3333	1807(1)	12(1)	1.70
B(1)	6750(6)	7654(6)	9301(7)	11(1)	3.07
B(2)	7847(6)	7491(6)	6596(6)	11(1)	3.10
B(3)	5863(7)	5356(7)	4778(6)	12(1)	3.05
O(1)	9199(4)	7726(4)	5714(3)	13(1)	2.00
O(2)	7221(4)	5479(4)	3909(3)	12(1)	2.03
O(3)	8056(4)	8119(4)	8076(3)	12(1)	2.13
O(4)	6186(4)	6483(4)	6013(4)	16(1)	2.13
O(5)	4196(4)	4203(4)	4498(4)	13(1)	1.90

Table S3. Selected bond lengths [Å] and angles [deg.] for α-$LiSrB_9O_{15}$.

Li(1)-O(1)	1.917(18)	B(3)-O(6)	1.451(7)
Li(1)-O(2)#4	2.133(14)	B(3)-O(9)	1.472(8)
Li(1)-O(6)#1	2.311(16)	B(4)-O(6)	1.357(7)
Li(1)-O(7)#5	1.983(13)	B(4)-O(7)	1.350(7)
Li(1)-O(11)#2	2.029(12)	B(4)-O(8)	1.404(7)
Li(1)-O(13)#3	2.203(11)	B(5)-O(8)	1.393(8)
Sr(1)-O(3)#1	2.602(4)	B(5)-O(9)	1.371(8)
Sr(1)-O(4)#1	2.870(4)	B(5)-O(10)	1.340(8)
Sr(1)-O(5)#6	2.493(4)	B(6)-O(2)#8	1.464(7)
Sr(1)-O(8)#3	2.823(4)	B(6)-O(5)#8	1.509(8)
Sr(1)-O(9)#6	2.518(4)	B(6)-O(10)	1.441(8)
Sr(1)-O(12)#3	2.754(4)	B(6)-O(11)	1.461(7)
Sr(1)-O(14)	2.437(3)	B(7)-O(11)	1.342(7)
Sr(1)-O(15)	2.737(4)	B(7)-O(12)	1.417(7)
B(1)-O(1)	1.342(8)	B(7)-O(13)	1.364(7)
B(1)-O(2)	1.363(7)	B(8)-O(7)#3	1.489(7)
B(1)-O(3)	1.388(7)	B(8)-O(13)	1.454(7)
B(2)-O(3)	1.382(7)	B(8)-O(14)	1.439(8)
B(2)-O(4)	1.342(7)	B(8)-O(15)#3	1.464(7)
B(2)-O(5)	1.379(8)	B(9)-O(12)	1.403(7)
B(3)-O(1)#7	1.478(7)	B(9)-O(14)	1.374(8)
B(3)-O(4)	1.450(8)	B(9)-O(15)	1.344(7)
O(2)#4-Li(1)-O(1)	146.0(7)	O(15)-Sr(1)-O(9)#6	88.10(13)
O(6)#1-Li(1)-O(1)	66.1(6)	O(15)-Sr(1)-O(12)#3	122.52(12)
O(6)#1-Li(1)-O(2)#4	86.3(4)	O(15)-Sr(1)-O(14)	52.16(14)
O(7)#5-Li(1)-O(1)	100.1(5)	O(2)-B(1)-O(1)	122.5(5)
O(7)#5-Li(1)-O(2)#4	113.8(9)	O(3)-B(1)-O(1)	118.5(5)
O(7)#5-Li(1)-O(6)#1	144.9(6)	O(3)-B(1)-O(2)	119.0(5)
O(11)#2-Li(1)-O(1)	104.6(6)	O(4)-B(2)-O(3)	113.4(5)
O(11)#2-Li(1)-O(2)#4	68.0(4)	O(5)-B(2)-O(3)	119.4(6)
O(11)#2-Li(1)-O(6)#1	114.3(5)	O(5)-B(2)-O(4)	127.2(6)
O(11)#2-Li(1)-O(7)#5	100.2(6)	O(4)-B(3)-O(1)#7	110.0(5)
O(13)#3-Li(1)-O(1)	107.4(6)	O(6)-B(3)-O(1)#7	105.3(5)
O(13)#3-Li(1)-O(2)#4	88.5(5)	O(6)-B(3)-O(4)	111.4(5)
O(13)#3-Li(1)-O(6)#1	85.2(4)	O(9)-B(3)-O(1)#7	110.1(5)
O(13)#3-Li(1)-O(7)#5	67.8(4)	O(9)-B(3)-O(4)	109.5(5)
O(13)#3-Li(1)-O(11)#2	147.2(10)	O(9)-B(3)-O(6)	110.4(5)
O(4)#1-Sr(1)-O(3)#1	48.87(12)	O(7)-B(4)-O(6)	118.2(5)
O(5)#6-Sr(1)-O(3)#1	91.58(13)	O(8)-B(4)-O(6)	119.9(5)
O(5)#6-Sr(1)-O(4)#1	97.35(13)	O(8)-B(4)-O(7)	121.8(5)
O(8)#3-Sr(1)-O(3)#1	172.12(13)	O(9)-B(5)-O(8)	119.6(6)
O(8)#3-Sr(1)-O(4)#1	133.46(12)	O(10)-B(5)-O(8)	124.3(6)
O(8)#3-Sr(1)-O(5)#6	80.72(13)	O(10)-B(5)-O(9)	115.9(5)
O(9)#6-Sr(1)-O(3)#1	67.68(13)	O(5)#8-B(6)-O(2)#8	110.1(5)
O(9)#6-Sr(1)-O(4)#1	115.35(13)	O(10)-B(6)-O(2)#8	107.2(5)

O(9)#6-Sr(1)-O(5)#6	70.59(14)	O(10)-B(6)-O(5)#8	109.7(5)
O(9)#6-Sr(1)-O(8)#3	107.77(13)	O(11)-B(6)-O(2)#8	105.4(5)
O(12)#3-Sr(1)-O(3)#1	121.22(13)	O(11)-B(6)-O(5)#8	111.0(5)
O(12)#3-Sr(1)-O(4)#1	74.71(12)	O(11)-B(6)-O(10)	113.2(5)
O(12)#3-Sr(1)-O(5)#6	79.11(13)	O(12)-B(7)-O(11)	120.2(5)
O(12)#3-Sr(1)-O(8)#3	59.17(12)	O(13)-B(7)-O(11)	120.5(5)
O(12)#3-Sr(1)-O(9)#6	148.89(13)	O(13)-B(7)-O(12)	119.2(5)
O(14)-Sr(1)-O(3)#1	117.17(13)	O(13)-B(8)-O(7)#3	105.4(5)
O(14)-Sr(1)-O(4)#1	91.94(12)	O(14)-B(8)-O(7)#3	111.4(5)
O(14)-Sr(1)-O(5)#6	147.80(14)	O(14)-B(8)-O(13)	111.2(4)
O(14)-Sr(1)-O(8)#3	70.70(12)	O(15)#3-B(8)-O(7)#3	109.3(4)
O(14)-Sr(1)-O(9)#6	131.80(14)	O(15)#3-B(8)-O(13)	109.4(5)
O(14)-Sr(1)-O(12)#3	73.74(14)	O(15)#3-B(8)-O(14)	110.0(5)
O(15)-Sr(1)-O(3)#1	76.06(13)	O(14)-B(9)-O(12)	119.5(5)
O(15)-Sr(1)-O(4)#1	87.94(12)	O(15)-B(9)-O(12)	125.6(5)
O(15)-Sr(1)-O(5)#6	158.30(13)	O(15)-B(9)-O(14)	114.9(5)
O(15)-Sr(1)-O(8)#3	110.70(12)		

Symmetry transformations used to generate equivalent atoms:

#1 x,y-1,z #2 -x+1/2,-y+1,z-1/2 #3 x+1/2,-y+1/2,-z+1 #4 -x+1,y-1/2,-z+3/2

#5 x+1/2,-y+3/2,-z+1 #6 x+1,y,z #7 x-1/2,-y+3/2,-z+1 #8 -x,y+1/2,-z+3/2

#9 x-1,y,z #10 -x+1/2,-y+1,z+1/2 #11 -x+1,y+1/2,-z+3/2 #12 -x,y-1/2,-z+3/2

#13 x-1/2,-y+1/2,-z+1 #14 x,y+1,z

Table S4. Selected bond lengths [Å] and angles [deg.] for α-$LiPbB_9O_{15}$.

Li(1)-O(3)#1	1.938(12)	Pb(1)-O(4)#10	2.716(3)
Li(1)-O(3)	1.938(12)	B(1)-O(5)#11	1.445(5)
Li(1)-O(3)#2	1.938(12)	B(1)-O(1)#5	1.458(6)
Li(1)-O(1)#3	2.220(15)	B(1)-O(3)	1.458(6)
Li(1)-O(1)#4	2.220(15)	B(1)-O(2)#5	1.516(5)
Li(1)-O(1)#5	2.220(15)	B(2)-O(1)	1.344(6)
Pb(1)-O(2)#6	2.479(3)	B(2)-O(3)	1.350(6)
Pb(1)-O(2)#7	2.479(3)	B(2)-O(4)	1.385(5)
Pb(1)-O(2)	2.479(3)	B(3)-O(5)	1.341(6)
Pb(1)-O(4)#8	2.716(3)	B(3)-O(2)	1.375(6)
Pb(1)-O(4)#9	2.716(3)	B(3)-O(4)	1.380(6)
O(3)#1-Li(1)-O(3)	99.5(8)	O(2)#6-Pb(1)-O(4)#9	87.89(10)
O(3)#1-Li(1)-O(3)#2	99.5(8)	O(2)#7-Pb(1)-O(4)#9	146.93(10)
O(3)-Li(1)-O(3)#2	99.5(8)	O(2)-Pb(1)-O(4)#9	74.61(9)
O(3)#1-Li(1)-O(1)#3	114.88(19)	O(4)#8-Pb(1)-O(4)#9	114.06(6)
O(3)-Li(1)-O(1)#3	144.4(3)	O(2)#6-Pb(1)-O(4)#10	146.93(10)
O(3)#2-Li(1)-O(1)#3	67.14(16)	O(2)#7-Pb(1)-O(4)#10	74.61(9)
O(3)#1-Li(1)-O(1)#4	67.14(16)	O(2)-Pb(1)-O(4)#10	87.89(10)
O(3)-Li(1)-O(1)#4	114.88(19)	O(4)#8-Pb(1)-O(4)#10	114.06(6)
O(3)#2-Li(1)-O(1)#4	144.4(3)	O(4)#9-Pb(1)-O(4)#10	114.06(6)
O(1)#3-Li(1)-O(1)#4	88.1(7)	O(5)#11-B(1)-O(1)#5	111.6(4)
O(3)#1-Li(1)-O(1)#5	144.4(3)	O(5)#11-B(1)-O(3)	109.6(3)
O(3)-Li(1)-O(1)#5	67.14(16)	O(1)#5-B(1)-O(3)	104.8(3)
O(3)#2-Li(1)-O(1)#5	114.88(19)	O(5)#11-B(1)-O(2)#5	108.8(3)
O(1)#3-Li(1)-O(1)#5	88.1(7)	O(1)#5-B(1)-O(2)#5	110.1(3)
O(1)#4-Li(1)-O(1)#5	88.1(7)	O(3)-B(1)-O(2)#5	112.1(4)
O(2)#6-Pb(1)-O(2)#7	73.92(10)	O(1)-B(2)-O(3)	121.8(4)
O(2)#6-Pb(1)-O(2)	73.92(10)	O(1)-B(2)-O(4)	119.2(4)
O(2)#7-Pb(1)-O(2)	73.92(10)	O(3)-B(2)-O(4)	118.9(4)
O(2)#6-Pb(1)-O(4)#8	74.61(9)	O(5)-B(3)-O(2)	124.2(4)
O(2)#7-Pb(1)-O(4)#8	87.89(10)	O(5)-B(3)-O(4)	116.1(4)
O(2)-Pb(1)-O(4)#8	146.93(10)	O(2)-B(3)-O(4)	119.7(4)

Symmetry transformations used to generate equivalent atoms:
#1 -y+2,x-y+1,z #2 -x+y+1,-x+2,z #3 -x+2,-y+2,z+1/2
#4 x-y+1,x,z+1/2 #5 y,-x+y+1,z+1/2 #6 -x+y+1,-x+1,z
#7 -y+1,x-y,z #8 y,-x+y,z-1/2 #9 x-y+1,x,z-1/2
#10 -x+1,-y+1,z-1/2 #11 -x+1,-y+1,z+1/2 #12 -x+2,-y+2,z-1/2

Figure S1. The coordination polyhedra of cations for (a, b) α-$LiSrB_9O_{15}$, (c, d) α-$LiPbB_9O_{15}$, (e, f) β-$LiSrB_9O_{15}$ and (g, h) β-$LiPbB_9O_{15}$.

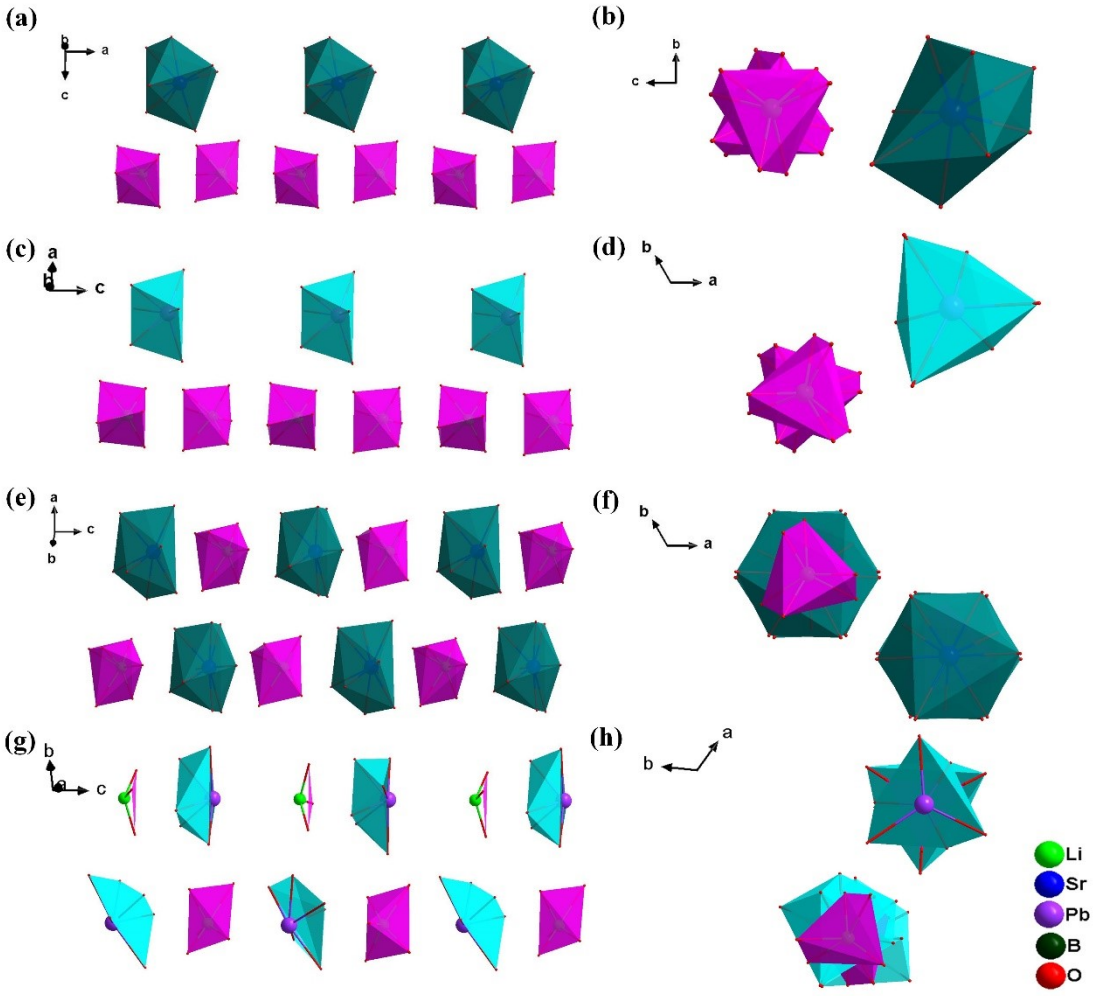

Figure S2. The FBUs connection mode of (a, c) α-$LiMB_9O_{15}$ (M = Sr, Pb) and (c, d) β-$LiMB_9O_{15}$ (M = Sr, Pb).

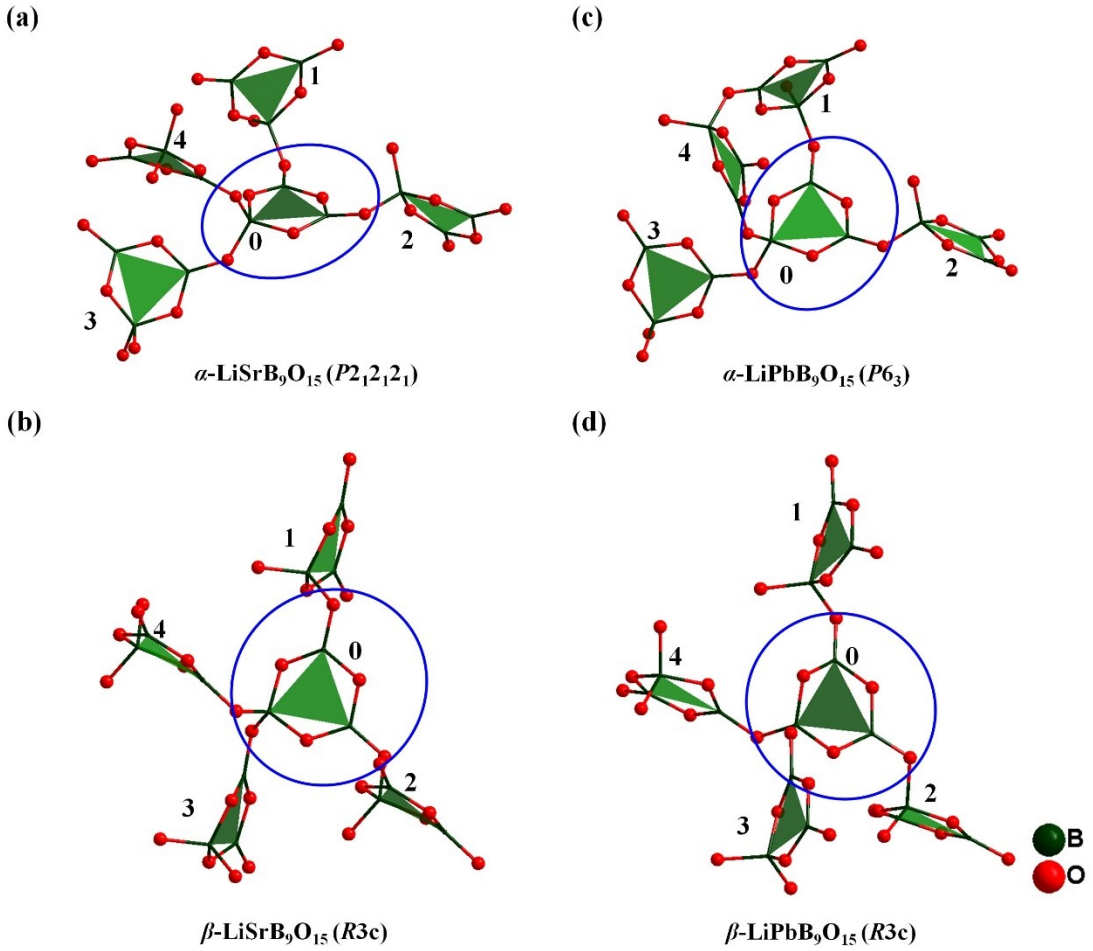

Table S5. The angles between the central plane (0) and surrounding four planes (1-4) constructed by three B atoms of $[B_3O_7]$ groups for α-$LiSrB_9O_{15}$, α-$LiPbB_9O_{15}$, β-$LiSrB_9O_{15}$, and β-$LiPbB_9O_{15}$.

	α-$LiSrB_9O_{15}$	α-$LiPbB_9O_{15}$	β-$LiSrB_9O_{15}$	β-$LiPbB_9O_{15}$
∠01	80.400 °	86.872 °	81.406 °	85.628 °
∠02	54.542 °	86.872 °	79.679 °	73.997 °
∠03	50.901 °	49.573 °	81.406 °	86.635 °
∠04	45.439 °	49.573 °	79.679 °	85.061 °

Table S6. Frameworks and FBUs of the known B_3O_5/B_6O_{10}/$B_{18}O_{30}$ class borates.

Compounds	Space groups	FBU	Anionic framework	CCDC
RbB_3O_5[7]	$P2_12_12_1$	$[B_3O_7]$	$^3[B_3O_5]_\infty$	91545
TlB_3O_5[8]	$P2_12_12_1$	$[B_3O_7]$	$^3[B_3O_5]_\infty$	84855
$Cs_2B_6O_{10}$[9]	$P2_12_12_1$	$[B_3O_7]$	$^3[B_3O_5]_\infty$	2081
KB_3O_5[10]	$P2_1/c$	$[B_3O_7]$	$^3[B_3O_5]_\infty$	250224
HP-TlB_3O_5[11]	$C2/c$	$[B_3O_8]$	$^3[B_3O_5]_\infty$	427689
HP-RbB_3O_5[12]	$C2/c$	$[B_3O_8]$	$^3[B_3O_5]_\infty$	424931
HP-KB_3O_5[13]	$C2/c$	$[B_3O_8]$	$^3[B_3O_5]_\infty$	423027
AgB_3O_5	$Pna2_1$	$[B_3O_7]$, $[B_3O_8]$	$^3[B_3O_5]_\infty$	428142
LiB_3O_5[14]	$Pna2_1$	$[B_3O_7]$	$^3[B_3O_5]_\infty$	1585
LiB_3O_5[15]	$Pnma$	$[BO_4]$, $[B_2O_5]$	$^3[B_3O_5]_\infty$	422922
CaB_6O_{10}[16]	$P2_1/c$	$[B_3O_7]$	$^3[B_3O_5]_\infty$	161320
$CsLiB_6O_{10}$[17]	$P222_1$	$[B_3O_7]$	$^3[B_3O_5]_\infty$	427409
$Na_3B_6O_{10}Cl$[18]	$P2_12_12_1$	$[B_6O_{13}]$	$^3[B_6O_{10}]_\infty$	251537
$RbNa_2B_6O_{10}Cl$[18]	$P2_12_12_1$	$[B_6O_{13}]$	$^3[B_6O_{10}]_\infty$	251539
$RbNa_2B_6O_{10}Br$[18]	$Pnma$	$[B_6O_{13}]$	$^3[B_6O_{10}]_\infty$	251538
$Na_3B_6O_{10}Br$[19]	$Pnma$	$[B_6O_{13}]$	$^3[B_6O_{10}]_\infty$	424557
$CsLiB_6O_{10}$[20]	$I\bar{4}2d$	$[B_3O_7]$	$^3[B_3O_5]_\infty$	75995
$K_3B_6O_{10}Cl$[21]	$R3m$	$[B_6O_{13}]$	$^3[B_6O_{10}]_\infty$	262005
$K_3B_6O_{10}Br$[22]	$R3m$	$[B_6O_{13}]$	$^3[B_6O_{10}]_\infty$	172400
$Na_2B_6O_{10}$[23]	$P2_1/c$	$[B_5O_{10}]$, $[BO_4]$ and $[B_3O_7]$	$^2[B_6O_{10}]_\infty$	2777
$Na_2Cs_2BaB_{18}O_{30}$[24]	$P2_1/c$	$[B_9O_{19}]$	$^3[B_{18}O_{30}]_\infty$	433333
$Na_2Cs_2PbB_{18}O_{30}$[24]	$P2_1/c$	$[B_9O_{19}]$	$^3[B_{18}O_{30}]_\infty$	433334
$Na_2Rb_2PbB_{18}O_{30}$[24]	$P2_1/c$	$[B_9O_{19}]$	$^3[B_{18}O_{30}]_\infty$	433335
$Na_2Cs_2SrB_{18}O_{30}$[25]	$P2_1/c$	$[B_9O_{19}]$	$^3[B_{18}O_{30}]_\infty$	193498
$Na_2Rb_2SrB_{18}O_{30}$[26]	$P2_1/c$	$[B_9O_{19}]$	$^3[B_{18}O_{30}]_\infty$	

Figure S3. The IR spectra of (a) α-$LiSrB_9O_{15}$ and (b) β-$LiSrB_9O_{15}$.

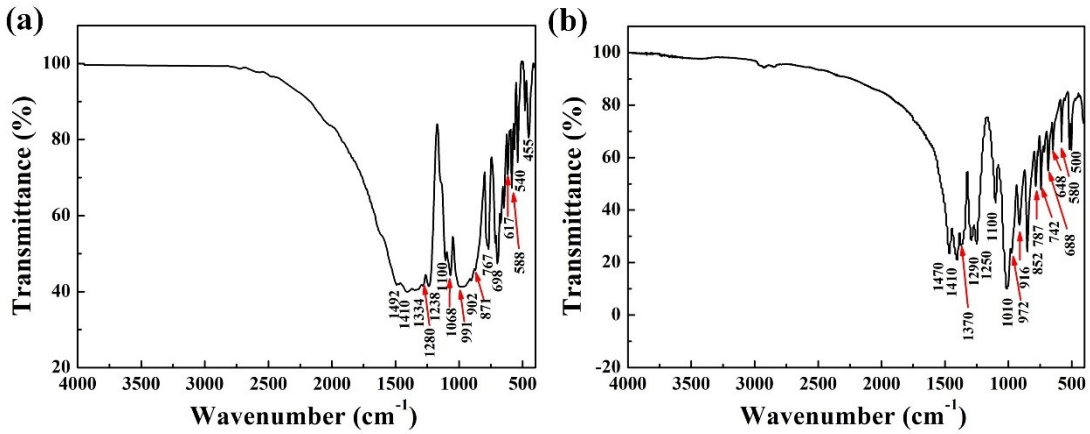

Figure S4. UV-vis-NIR diffuse reflectance spectra of (a) α-$LiSrB_9O_{15}$ and (b) β-$LiSrB_9O_{15}$.

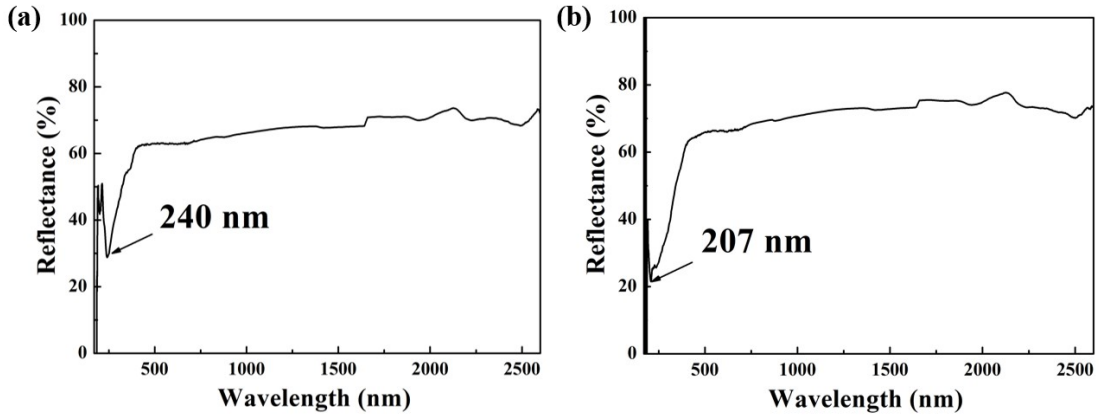

Table S7. Comparison of observed IR absorption peaks (cm^{-1}) of α-$LiSrB_9O_{15}$ and β-$LiSrB_9O_{15}$ with literature assignments.

Mode description	α-$LiSrB_9O_{15}$	β-$LiSrB_9O_{15}$
Asymmetric stretching of B-O in the [BO_3]	1492, 1410, 1334, 1238, 1100	1470, 1410, 1370, 1290, 1250, 1100
Asymmetric stretching of B-O in the [BO_4]	1060	1010
Symmetric stretching of B-O in the [BO_3]	991, 902	972, 916
Symmetric stretching of B-O in the [BO_4]	871	852
Bending vibrations of B-O in the [BO_3]	767, 698, 617	742, 720, 688
Symmetric pulse vibration of the [BO_3]	588	580
Bending modes of [BO_4] and [BO_3]	540, 455	500

Figure S5. Band structures (a) and PDOS (b) of α-$LiPbB_9O_{15}$.

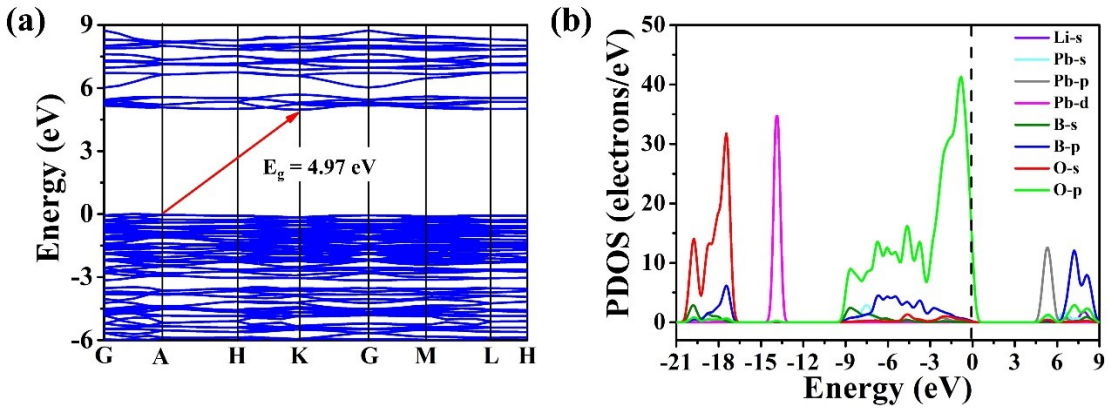

Figure S6. The [BO_3] triangles arrangements of (a, b, c) α- and (d, e, f) β-$LiSrB_9O_{15}$ from different orientations.

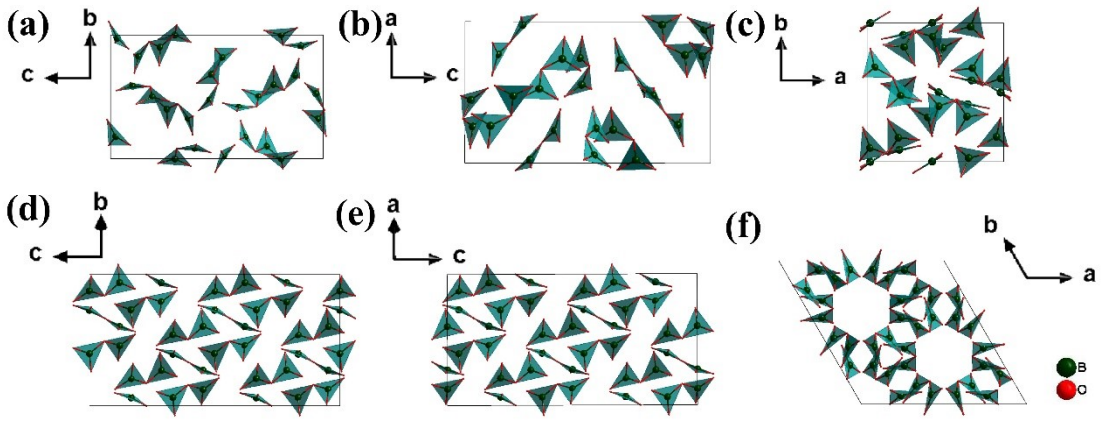

Uncategorized References

1. G. Sheldrick, SHELXT - Integrated Space-Group and Crystal-Structure Determination, *Acta Crystallogr. A*, 2015, **71**, 3-8.
2. A. L. Spek, Single-Crystal Structure Validation with the Program PLATON, *J. Appl. Crystallogr.*, 2003, **36**, 7-13.
3. S. J. Clark, M. D. Segall, C. J. Pickard, P. J. Hasnip, M. J. Probert, K. Refson and M. C. Payne, First-Principles Methods Using CASTEP, *Z. Kristallogr. - Cryst. Mater.*, 2005, **220**, 567-570.
4. J. P. Perdew, K. Burke and M. Ernzerhof, Generalized Gradient Approximation Made Simple, *Phys. Rev. Lett.*, 1996, **77**, 3865-3868.
5. A. M. Rappe, K. M. Rabe, E. Kaxiras and J. D. Joannopoulos, Optimized pseudopotentials, *Phys. Rev. B*, 1990, **41**, 1227.
6. J. S. Lin, A. Qteish, M. C. Payne and V. Heine, Optimized and Transferable Nonlocal Separable *ab* Initio Pseudopotentials, *Phys. Rev. B*, 1993, **47**, 4174-4180.
7. M. G. Krzhizhanovskaya, Y. K. Kabalov, R. S. Bubnova, E. V. Sokolova and S. K. Filatov, Crystal Structure of the Low Temperature Modification α-(RbB_3O_5), *Kristallogr.*, 2000, **45**, 629-634.
8. M. Touboul, E. Bétourné and G. Nowogrocki, Crystal Structure of Thallium Triborate, TlB_3O_5, *J. Solid State Chem.*, 1997, **131**, 370-373.
9. J. Krogh-Moe, Refinement of the Crystal Structure of Caesium Triborate, $Cs_2O.3B_2O_3$, *Acta Crystallogr. B*, 1974, **30**, 1178-1180.
10. R. S. Bubnova, V. S. Fundamenskii, S. K. Filatov and I. G. Polyakova, Crystal Structure and Thermal Behavior of KB_3O_5, *Dokl. Phys. Chem.*, 2004, **398**, 249-253.
11. G. Sohr, L. Perfler and H. Huppertz, The High-Pressure Thallium Triborate HP-TlB_3O_5, *Z. Naturforsch. B*, 2014, **69**, 1260-1268.
12. G. Sohr, S. C. Neumair and H. Huppertz, High-Pressure Synthesis and Characterization of the Alkali Metal Borate HP-RbB_3O_5, *Z. Naturforsch. B*, 2012, **67**, 1197-1204.
13. S. C. Neumair, S. Vanicek, R. Kaindl, D. M. Többens, C. Martineau, F. Taulelle, J. Senker and H. Huppertz, HP-KB_3O_5 Highlights the Structural Diversity of Borates: Corner-Sharing BO_3/BO_4 Groups in Combination with Edge-Sharing BO_4 Tetrahedra, *Eur. J. Inor. Chem.*, 2011, **2011**, 4147-4152.
14. H. König and R. Hoppe, Über Borati der Alkalimetalle. II. Zur Kenntnis von LiB_3O_5 [1], *Z. Anorg. Allg. Chem.*, 1978, **439**, 71-79.
15. S. C. Neumair, S. Vanicek, R. Kaindl, D. M. Többens, K. Wurst and H. Huppertz, High-Pressure Synthesis and Crystal Structure of the Lithium Borate HP-LiB_3O_5, *J. Solid State Chem.*, 2011, **184**, 2490-2497.
16. X. Chen, M. Li, X. Chang, H. Zang and W. Xiao, Synthesis and Crystal Structure of a New Calcium Borate, CaB_6O_{10}, *J. Alloys Compd.*, 2008, **464**, 332-336.
17. N. A. Sennova, G. Cordier, B. Albert, S. K. Filatov, R. S. Bubnova, L. I. Isaenko, L. I. Gubenko, J.-P. Klöckner and M. H. Prosenc, Temperature- and Moisture-Dependency of $CsLiB_6O_{10}$. A New Phase, β-$CsLiB_6O_{10}$, *Z. Kristallogr. - Cryst. Mater.*, 2014, **229**, 741-751.
18. C. Y. Bai, H. W. Yu, S. J. Han, S. L. Pan, B. B. Zhang, Y. Wang, H. P. Wu and Z. H. Yang, Effect of Halogen (Cl, Br) on the Symmetry of Flexible Perovskite-Related Framework, *Inorg. Chem.*, 2014, **53**, 11213-11220.
19. Z. H. Chen, S. L. Pan, X. Y. Dong, Z. H. Yang, M. Zhang and X. Su, Exploration of a New

Compound in the M–B–O–X (M: Alkali Metals; X: Halogen) System: Preparation, Crystal and Electronic Structures, and Optical Properties of $Na_3B_6O_{10}Br$, *Inorg. Chim. Acta*, 2013, **406**, 205-210.

20. J.-M. Tu and D. A. Keszler, $CsLiB_6O_{10}$: A Noncentrosymmetric Polyborate, *Mater. Res. Bull.*, 1995, **30**, 209-215.
21. H. P. Wu, S. L. Pan, K. R. Poeppelmeier, H. Y. Li, D. Z. Jia, Z. H. Chen, X. Y. Fan, Y. Yang, J. M. Rondinelli and H. S. Luo, $K_3B_6O_{10}Cl$: A New Structure Analogous to Perovskite with a Large Second Harmonic Generation Response and Deep UV Absorption Edge, *J. Am. Chem. Soc.*, 2011, **133**, 7786-7790.
22. A. G. Al'-Ama, E. L. Belokoneva, S. Y. Stefanovich, O. V. Dimitrova and N. N. Mochenova, Potassium Bromo-Borate $K_3[B_6O_{10}]Br$ - a New Nonlinear Optical Material, *Kristallogr.*, 2004 254-258.
23. J. Krogh-Moe, The Crystal Structure of a Sodium Triborate Modification, β-$Na_2O.3B_2O_3$, *Acta Crystallogr. B*, **28**, 1571-1576.
24. M. Mutailipu, M. Zhang, X. Su, Z. H. Yang, Y. N. Chen and S. L. Pan, Structural Insights into Borates with an Anion-Templated Open-Framework Configuration: Asymmetric $K_2BaB_{16}O_{26}$ versus Centrosymmetric $K_3CsB_{20}O_{32}$ and $Na_2M_2NB_{18}O_{30}$ (M=Rb, Cs; N=Ba, Pb), *Chem. Eur. J.*, 2017, **23**, 13910-13918.
25. X. A. Chen, L. Wu, K. Wang, X. A. Chang and W. Q. Xiao, Synthesis and Characterization of a New Quaternary Borate $Na_2Cs_2Sr(B_9O_{15})_2$ with the Unprecedented $[B_9O_{19}]^{11-}$ Group, Notation of 3×(3:2Δ+T), *J. Alloys Compd.*, 2015, **623**, 157-163.
26. J. J. Zheng, T. Zhang, J. W. Feng, D. H. An, C. Y. Bai and Y. Sun, $Na_2Rb_2SrB_{18}O_{30}$ with $[B_9O_{19}]^{11-}$ Fundamental Building Block Consisting of Three $[B_3O_7]^{5-}$ Groups, *Z. Anorg. Allg. Chem.*, 2021, **647**, 1578-1582.